energies

MDPI

Article

Time–Frequency Domain Signal Analysis for Knock Detection in Hydrogen-Fueled Engines

Brijesh Kinkhabwala *, Uwe Wagner and Thomas Koch

Institute of Internal Combustion Engines (IFKM), Karlsruhe Institute of Technology (KIT), 76131 Karlsruhe, Germany; uwe.wagner@kit.edu (U.W.); thomas.a.koch@kit.edu (T.K.)
* Correspondence: brijesh.kinkhabwala@kit.edu

Abstract

Hydrogen is a promising carbon-neutral fuel for future internal combustion engines due to its wide flammability range, high flame speed, and absence of carbon-based emissions. However, its high reactivity significantly increases susceptibility to abnormal combustion phenomena such as knock and pre-ignition, which can compromise engine efficiency, durability, and operational stability. Accurate detection and characterization of knock in hydrogen-fueled spark-ignition engines remain challenging due to the highly transient, broadband, and cycle-dependent nature of abnormal combustion-induced pressure oscillations. Conventional knock indicators based solely on time-domain pressure oscillations or fixed-band frequency analysis are limited in their ability to capture transient resonance behavior and cyclic variability. This study presents an integrated frequency- and time–frequency-domain methodology for knock detection using high-resolution in-cylinder pressure data acquired from a single-cylinder research engine operating under hydrogen port fuel injection (PFI). A discrete Fast Fourier Transform (DFFT) approach applied at stationary points of dynamically windowed pressure signals enables accurate identification of dominant resonance modes while minimizing spectral leakage. A Gaussian-based adaptive windowing strategy is introduced to capture combustion-driven cyclic variations more effectively. Short-Time Fourier Transform (STFT) and sum-based spectral analysis further provide detailed time–frequency localization of transient knock events. The proposed methodology demonstrates a clear separation between normal combustion and knock conditions, enabling reliable cycle-by-cycle identification of abnormal combustion events under varying operating conditions. The experimentally observed resonance frequencies are validated against theoretical predictions using Draper's acoustic resonance equation, supporting the physical interpretation of knock-induced pressure oscillations. The results demonstrate that the proposed adaptive spectral methodology significantly improves knock detection accuracy compared to conventional indicators and provides a robust framework for advanced knock diagnostics, engine calibration, and combustion control in hydrogen-fueled engines.

Keywords: hydrogen combustion; knock detection; pre-ignition; FFT; STFT; time–frequency analysis; in-cylinder pressure oscillations

Academic Editor: Constantine D. Rakopoulos

Received: 15 April 2026
Revised: 29 May 2026
Accepted: 29 May 2026
Published: 4 June 2026

1. Introduction

The global energy crisis, driven by the depletion of fossil fuels and growing environmental concerns, has intensified the search for cleaner energy alternatives. Road vehicles, which rely heavily on fossil fuel combustion, contribute approximately 16% of global CO_2

emissions, while conventional internal combustion engines (ICEs) emit harmful pollutants such as unburned hydrocarbons, nitrogen oxides (NOx), CO, and particulate matter (PM), negatively impacting both the environment and human health [1]. To mitigate these effects, strict emission regulations have been implemented worldwide, prompting investigations into renewable and low-emission fuels. Among these, hydrogen has emerged as a particularly promising option for transportation, being a renewable, carbon-free fuel that produces primarily water and trace NOx during combustion [2,3]. Hydrogen is especially suitable for spark ignition (SI) engines due to its high auto-ignition temperature, high calorific value, low density, rapid flame propagation, and wide flammability range. These properties enable efficient lean combustion, improved thermal efficiency, and rapid mixing, which can reduce emissions and enhance engine performance compared to conventional fuels [4,5]. However, hydrogen's extremely low ignition energy (~0.02 mJ) and wide flammability range make engines prone to knock, which remains a critical barrier to its broader adoption [6]. Knock in hydrogen engines manifests as sharp acoustic pressure oscillations caused primarily by auto-ignition of the unburned end-gas, producing rapid heat release that can amplify pressure waves and damage engine components [7]. Interestingly, light knock can also arise from combustion instabilities without full auto-ignition, while heavy knock generally results from end-gas auto-ignition [8].

The ultrafast flame speed of hydrogen and its detonation-prone nature under stoichiometric conditions further exacerbate knock occurrence, as the interaction between pressure waves and the flame front can amplify combustion instabilities [9]. Determining the precise onset of knock remains a challenge for engine calibration. Previous studies have investigated combinations of existing knock indices to develop more robust indicators that are easier to apply across different engine settings. For instance, the ratio of the Integral of Modulus of Pressure Oscillation (IMPO) to the product of Maximum Amplitude of Pressure Oscillation (MAPO) and the window width (W) has been proposed as an effective knock indicator, providing accurate prediction of knock-limited spark advance independent of fuel composition [10]. Building upon this, recent work has emphasized the advantages of time–frequency- and frequency-domain analysis for knock characterization. A new knock index has been proposed that compares the excitation of cylinder resonance caused by end-gas autoignition to that of normal combustion, using Fast Fourier Transform (FFT) applied near the peak heat release and the end of combustion. This index has been shown to reduce variability in spark advance control and improve differentiation between knocking and non-knocking cycles compared to classical MAPO-based methods [11]. In addition, previous studies on hydrogen port fuel injection engines operating at high engine speeds demonstrated that FFT analysis can effectively identify hydrogen-specific knock characteristics, including higher resonance frequencies compared to gasoline engines and distinct propagation behavior between light and heavy knock conditions. These studies also highlighted the strong influence of ignition timing and backfire on abnormal combustion development in hydrogen engines, further emphasizing the importance of frequency-domain analysis for accurate knock characterization and combustion diagnosis [12].

Furthermore, advanced frequency-domain approaches such as the Selective Sampling Filtration (SSF) method have been developed to enhance knock detection accuracy. By isolating the contribution of dominant knock-sensitive frequency bands from pressure signals, SSF effectively separates knock-induced oscillations from background noise and broadband combustion fluctuations. Experimental studies have demonstrated that applying band-pass filtering techniques to the cylinder pressure and vibration signals, followed by non-dimensional evaluation of knock intensity, provides a universal threshold for knock detection that is robust against sensor location and engine operating conditions [13]. Such methods are particularly relevant for hydrogen-fueled engines, where high cycle-to-cycle

variability and multiple resonance modes necessitate precise spectral analysis to quantify knock amplitude and improve control strategies.

Despite these advances, conventional knock detection methods often fail to capture the transient and cycle-dependent nature of knock in hydrogen engines, limiting their reliability for accurate diagnosis and control. Therefore, the present study investigates knock phenomena in a hydrogen-fueled research engine using an integrated frequency-domain analysis framework. In this work, discrete Fast Fourier Transform (DFFT) applied to dynamically windowed pressure signals is used to accurately identify dominant resonance modes while minimizing spectral distortion and leakage effects. The experimentally observed resonance frequencies are further compared with theoretical predictions based on Draper's acoustic resonance equation to establish their physical relevance.

In addition, Short-Time Fourier Transform (STFT), a widely adopted time–frequency analysis technique for combustion diagnostics and knock characterization [11,14–17], is employed as a supporting analysis tool to visualize the temporal evolution of knock-induced oscillations and cyclic variations. Previous studies have shown that STFT can effectively distinguish knock-induced resonance behavior from mechanical noise by analyzing both the frequency content and its temporal attenuation characteristics [17]. Furthermore, STFT-based approaches have been successfully applied to identify combustion excitation, valve impacts, piston slap, and knock-related vibration events in internal combustion engines [15,17]. Compared to direct DFFT analysis, STFT provides improved localization of transient combustion phenomena in both time and frequency domains [15]. Earlier investigations also demonstrated that combining STFT with FFT-based resonance analysis improves the identification of low-intensity knock cycles and reduces variability in knock-related combustion control [11]. Conventional STFT implementations generally rely on fixed window lengths and locations; however, due to the highly transient nature and strong cycle-to-cycle variability of hydrogen combustion, selecting a single fixed window size can lead to signal loss or inaccurate localization of abnormal combustion events. Therefore, in the present work, a dynamically adapted Gaussian windowing strategy is introduced to better capture combustion-dependent variations while minimizing spectral leakage and preserving resonance characteristics. The primary focus of this study, however, remains on the development of an improved FFT-based knock quantification methodology incorporating adaptive window selection and inverse FFT reconstruction for accurate knock amplitude estimation. Through this approach, this study provides deeper insight into the spectral characteristics, resonance behavior, and detection reliability of knock in hydrogen combustion, contributing to more robust diagnostic and control methodologies for advanced hydrogen engines.

2. Experimental Setup

The experiments were conducted on a single-cylinder, four-stroke spark-ignition research engine with a displacement of 2.5 L as shown in Figure 1. The engine was equipped with a flat-roof cylinder head and a four-valve configuration (two intake and two exhaust valves). The original diesel-based engine was retrofitted to operate with hydrogen fuel using a PFI injection setup. The engine was operated under steady-state conditions using an eddy-current dynamometer to precisely control engine speed and load. The engine was installed in a fully instrumented test cell equipped with high-speed combustion measurement and control systems. In-cylinder pressure was measured using a Kistler piezoelectric pressure transducer (high-frequency piezoelectric Kistler transducer (featuring a linearity of $\leq \pm 0.3\%$ FSO) mounted flush with the cylinder head to capture high-frequency pressure variations. The pressure signal was acquired at high crank-angle resolution using an AVL INDIMASTER Advanced data acquisition system, enabling cycle-

resolved pressure measurement for detailed combustion and knock analysis. Typically, 1000 consecutive engine cycles were recorded for each operating condition to ensure statistically reliable analysis.

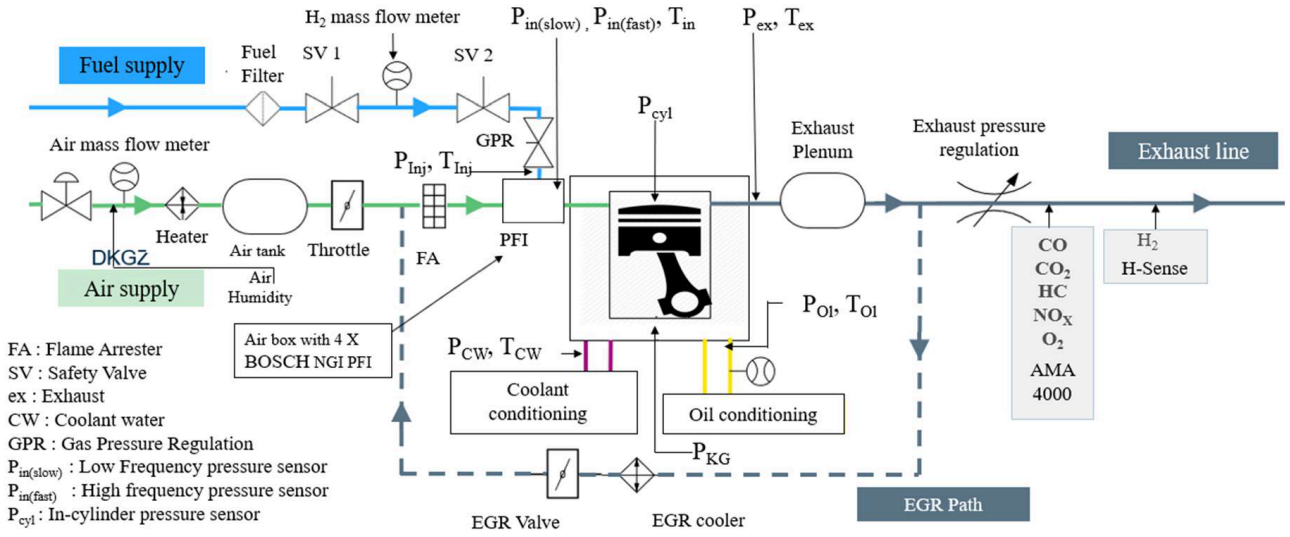

Figure 1. Engine architecture showing sensor, actuator, and measurement locations.

The acquired in-cylinder pressure data were used for both real-time monitoring and detailed offline post-processing. The high-frequency response of the pressure measurement system enabled accurate capture of combustion-induced pressure oscillations associated with knock and abnormal combustion events. To ensure safe operation during knock-prone hydrogen combustion, a real-time safety mechanism was implemented using the AVL INDIMASTER combustion analysis system integrated with the MORPHEE test cell control platform. When the measured in-cylinder pressure exceeded a predefined maximum pressure threshold, or when an abnormal increase in the maximum pressure rise rate was detected, the INDIMASTER system immediately transmitted a shutdown signal to the MORPHEE control system. This triggered an instantaneous cutoff of the hydrogen fuel supply, preventing potential engine damage due to excessive knock or uncontrolled pressure rise. The safety logic was based on fundamental knock-related parameters, specifically the maximum in-cylinder pressure and the maximum pressure rise rate, which served as primary indicators of abnormal combustion severity. The engine was operated under knock-prone conditions to enable detailed investigation of abnormal combustion characteristics. In addition, an H_2 sensor was installed at the engine exhaust line to continuously monitor potential hydrogen leakage into the exhaust system, ensuring safe operation and preventing fire hazards or unintended hydrogen combustion within the exhaust after-treatment facility. The subject engine selected for this study was a heavy-duty single-cylinder research engine with a bore of 140 mm, a stroke of 170 mm, and a compression ratio of 12:1. The selected operating condition corresponded to an engine speed of 1100 rpm, an indicated mean effective pressure (IMEP) of 18 bar, and an excess air ratio lambda (λ) of 2.2. A constant lambda condition was maintained using a closed-loop monitoring and control strategy, where the continuous oxygen concentration was measured using an EMA 4000 analyzer and the air–fuel ratio was regulated through automated air and fuel actuation within the test-cell control system.

The spark timing was selected such that the center of combustion remained close to top dead center (TDC), creating favorable thermodynamic conditions for the occurrence and investigation of knock phenomena. The combination of relatively advanced combustion phasing, a high compression ratio, and elevated load promoted combustion anomalies,

particularly pressure oscillations and knock-related behavior. These operating conditions were therefore considered representative of highly loaded hydrogen combustion with increased susceptibility to abnormal combustion phenomena. The overall experimental setup provided a reliable and controlled platform for acquiring high-resolution in-cylinder pressure data required for accurate time-domain and frequency-domain knock analysis.

3. Conventional Knock Indicators

The detection and quantification of knock in internal combustion engines have traditionally relied on several pressure-based indicators derived from high-resolution in-cylinder pressure measurements. These conventional knock indicators are primarily calculated in the time domain and provide valuable information about combustion intensity, pressure rise rate, and oscillatory behavior associated with abnormal combustion. In this study, the in-cylinder pressure signal is used as the primary diagnostic input to evaluate knock intensity using multiple established parameters, as shown in Table 1 with their physical significance, comparison and formulation. Each of these indicators captures a different physical aspect of the combustion process, including peak pressure magnitude, pressure oscillation amplitude, pressure gradient behavior, and heat release characteristics. Although these indicators have been widely used in conventional gasoline and diesel engines, their applicability to hydrogen combustion requires careful evaluation due to hydrogen's rapid combustion characteristics and higher susceptibility to pressure oscillations. Each individual indicator was calculated over 1000 cycle data and is plotted over cycle number in Figure 2. Although conventional knock indicators provide useful information, they have several limitations when applied to hydrogen combustion. Hydrogen combustion produces higher frequency oscillations and greater cycle-to-cycle variability compared to conventional fuels. As a result, time-domain indicators alone cannot fully characterize knock behavior, particularly when knock events are intermittent or contain multiple frequency components. Additionally, these indicators do not provide information about the specific resonance frequencies associated with knock, making it difficult to distinguish combustion-induced oscillations from structural or sensor-related noise.

Table 1. Conventional knock indicators.

Conventional Knock Indicators	Physical Significance and Comparison	Formulation
Heat Release Rate (HRR)	Derived from the first law of thermodynamics, HRR provides insight into the rate of energy release during combustion. Abnormal spikes or irregular patterns indicate knock or pre-ignition. Key parameters: γ = ratio of specific heats, V(θ) = cylinder volume, this might not be the absolute indicator for hydrogen combustion, as a reduction in heat release can also result from misfire, pre-ignition, or general combustion inefficiency.	$\left(\frac{dQ}{d\theta}\right) = \left(\frac{\gamma}{\gamma-1}\right)P(\theta)\left(\frac{dV}{d\theta}\right) + \left(\frac{1}{\gamma-1}\right)V(\theta)\left(\frac{dP}{d\theta}\right)$
Maximum In-Cylinder Pressure (Pmax)	Represents the peak pressure during a combustion cycle. Useful as a first-level indicator for abnormal combustion and engine protection (e.g., shutdown safety). Under knocking conditions, Pmax increases due to rapid energy release. However, high Pmax alone cannot reliably distinguish knock from high-load normal combustion.	$P_{max} = \max(P(\theta))$ P(θ) = instantaneous cylinder pressure

Table 1. *Cont.*

Conventional Knock Indicators	Physical Significance and Comparison	Formulation
Maximum Amplitude of Pressure Oscillation (MAPO)	Measures the maximum amplitude of high-frequency pressure oscillations superimposed on the main combustion pressure. Directly reflects knock intensity and is more sensitive than Pmax. This absolute value includes contributions from the knock frequency as well as the natural frequencies of the pressure sensor and other engine components; therefore, the measured value can often appear significantly higher than the actual knock intensity.	$P_{osc}(\theta) = P(\theta) - P_{smooth}(\theta)$ $P_{osc}(\theta)$ = oscillating pressure component $P_{smooth}(\theta)$ = low-pass filtered or smoothed pressure signal $A_{osc} = \max(\lvert P_{osc(\theta)} \rvert)$ A_{osc} = knock oscillation amplitude
Maximum Pressure Rise Rate	Represents the steepest pressure increase per crank angle. Rapid pressure rise indicates fast combustion or auto-ignition. Knock typically produces higher rise rates compared to normal combustion, though fast normal combustion can also increase this value. Inhomogeneity in the fuel–air mixture can also lead to spikes in the maximum pressure rise rate; therefore, this parameter alone may limit the accurate identification of knock onset.	$\left(\frac{dP}{d\theta}\right)_{max} = \max\left[\frac{dP(\theta)}{d\theta}\right]$
Integral of Modulus of Pressure Gradient (IMPG)	Cumulative measure of the magnitude of pressure gradients over a defined crank angle range. High IMPG values indicate aggressive combustion and potential knock occurrence.	$IMPG = \int_{\theta_1}^{\theta_2} \left\lvert \frac{dP(\theta)}{d\theta} \right\rvert d\theta$
Integral of Modulus of Pressure Oscillation (IMPO)	Measures total oscillatory energy over a crank angle interval. Provides a quantitative measure of knock energy and captures oscillation effects missed by single-point amplitude measurements.	$IMPO = \int_{\theta_1}^{\theta_2} \left\lvert P_{osc(\theta)} \right\rvert d\theta$
Derivative Knock Index (DKI)	The Derivative Knock Index (DKI) is a dimensionless knock indicator that quantifies the normalized cumulative intensity of the oscillatory pressure component within the knock window. Higher DKI values indicate sustained and energetically significant knock oscillations, providing a robust measure of knock severity that accounts for both amplitude and duration of pressure oscillations. The results for hydrogen combustion using this parameter show fully scattered behavior due to higher oscillation; hence, it is difficult to use it for knock detection.	$\mathrm{DKI} = \frac{\int_{\theta_1}^{\theta_2} \lvert \hat{P}(\theta) \rvert \, d\theta}{\mathrm{MAPO} \cdot \zeta}$ ζ = normalization constant Defined as the ratio of the integral of the absolute oscillating pressure to the Maximum Amplitude of Pressure Oscillation (MAPO), scaled by a normalization factor ζ.

Furthermore, due to the inherently fast combustion rate and high cycle-to-cycle variability of hydrogen combustion, knock-related parameters such as IMPG, IMPO, and DKI exhibit increased cycle-to-cycle fluctuations even under normal combustion conditions. These variations are primarily observed in the pressure oscillation signal and derived knock indices, rather than in a single deterministic combustion signature, which complicates the direct identification of knock onset based solely on time-domain metrics.

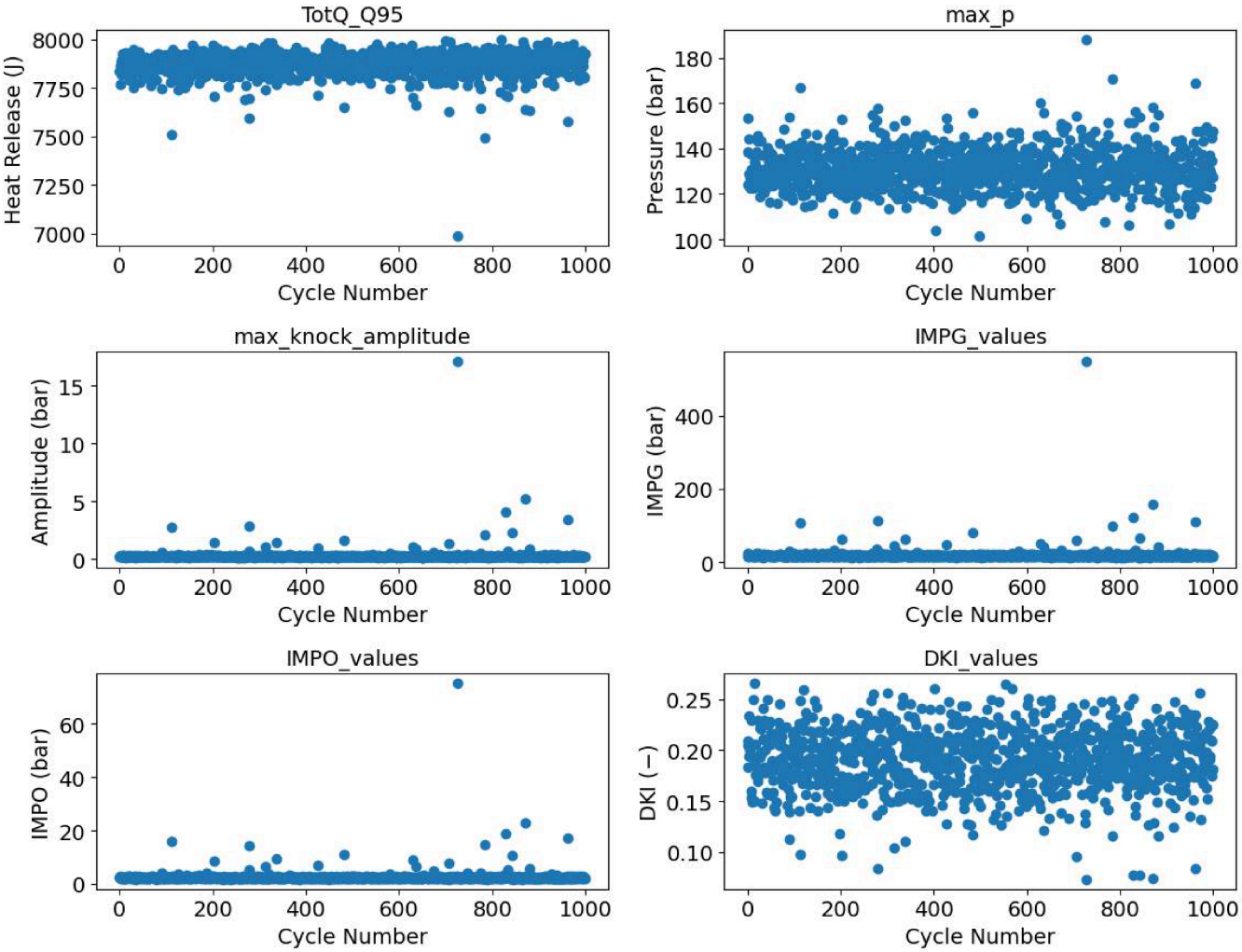

Figure 2. Comparison of conventional knock indicators plotted for overall evaluation and correlation analysis.

Additionally, these indicators integrate overall pressure gradient and oscillation energy without isolating specific resonance frequencies, making them less reliable for accurately distinguishing true knock events from normal combustion-induced pressure fluctuations in hydrogen engines. Therefore, while conventional knock indicators remain useful for preliminary knock detection and comparison, more advanced analysis techniques such as frequency-domain and time–frequency-domain analysis are required for accurate knock characterization in hydrogen-fueled engines. The following sections present advanced methodologies based on Fourier Transform analysis to overcome these limitations and provide more reliable knock detection.

4. Online and Offline Knock Detection Methodologies

Knock detection in hydrogen-fueled engines can be performed using both online (real-time) and offline (post-processing) analysis methods. Online knock detection is carried out during engine operation using combustion analysis systems such as AVL IndiCom or INDIMASTER, which continuously acquire in-cylinder pressure data and calculate knock indicators for each cycle. The primary purpose of online detection is to identify knock onset immediately and enable corrective control actions to protect engine hardware. However, online methods are limited by real-time processing constraints, reduced signal

resolution, and sensitivity to noise, which can lead to incomplete characterization of transient knock features.

In most cases, conventional knock parameters are used for online calculation due to their simplicity and fast processing capability. However, when using AVL combustion analysis systems, the built-in knock detection parameter can be utilized, which has been shown in previous studies to correlate well with knock onset [18]. One of the most commonly used online knock indicators is the Peak Knock Parameter, denoted KP_PK. The KP_PK analysis involves a two-step procedure. First, a running average of the pressure signal is computed to remove high-frequency oscillations and obtain a smoothed baseline pressure signal. This step ensures that normal combustion trends are separated from knock-induced pressure fluctuations. Second, the Knock Index (KI) is determined as the local maximum difference between the actual pressure signal and the smoothed pressure signal. Although KP_PK is a reliable online knock indicator, it cannot always accurately determine knock amplitude, location, or duration, making it difficult to identify knock onset based solely on this parameter.

Single knocking parameters, including KP_PK, maximum pressure rise, and oscillation amplitude, can yield inconsistent values across varying operating conditions, and instances exist where high KP_PK values do not correspond to high maximum pressure, and vice versa. As shown in the figure above, the MAPO and KP_PK graphs do not always match; the left side of Figure 3 shows knock intensity measured using MAPO, which differs significantly from the KP_PK values. Other conventional online indicators, such as pressure rise rate and oscillation integrals, face similar limitations due to the high cycle-to-cycle variability of hydrogen combustion and real-time computational constraints, sometimes resulting in missed or misidentified knock events. Offline post-processing using Python v3.10.7—based analysis allows incorporation of additional combustion parameters (CA05, CA10, CA50, CA95, IMEP) and advanced signal processing techniques such as FFT and time–frequency analysis, improving detection reliability and physically meaningful identification of knock events. In this study, offline analysis validates and enhances knock detection beyond conventional online methods. As shown in Figure 4, the FFT amplitude at a particular knock frequency over 1000 cycles aligns closely with the most reliable online knock indicator, confirming the correlation between frequency-domain analysis and conventional online measurements.

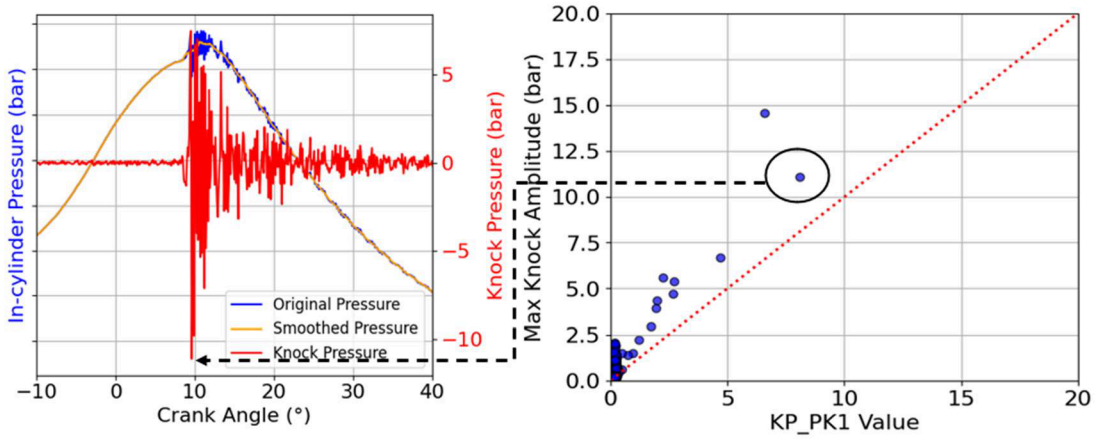

Figure 3. (**Left**)—Maximum Amplitude of Pressure Oscillation (MAPO); (**Right**)—correlation between KP-PK and MAPO over 1000 consecutive combustion cycles.

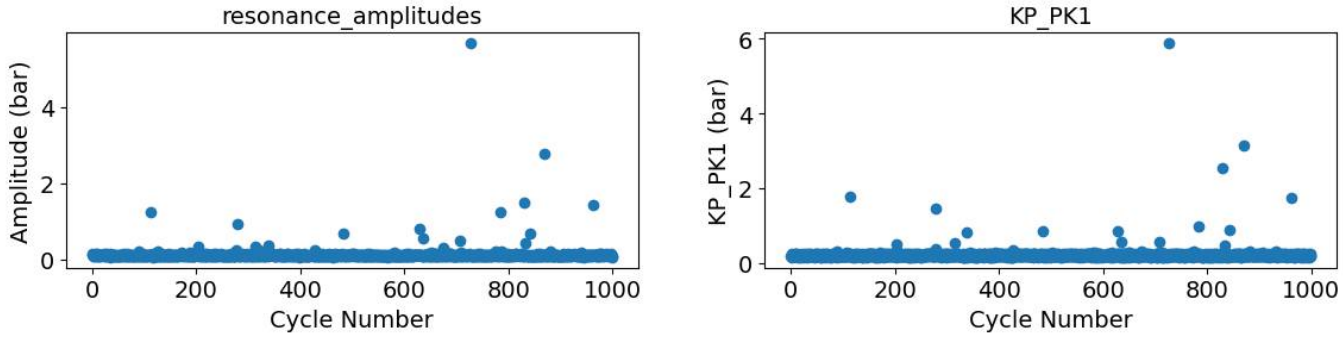

Figure 4. (**Left**)—offline FFT amplitude calculation for knock detection; (**Right**)—online KP-PK knock indicator for all 1000 cycles.

5. Frequency-Domain Knock Analysis Using Fast Fourier Transform (FFT)

Conventional time-domain knock indicators provide useful information about combustion intensity but do not provide insight into the frequency characteristics of knock. However, knock is fundamentally an acoustic resonance phenomenon that occurs at specific natural frequencies of the combustion chamber. These pressure oscillations are generated by rapid energy release and propagate as acoustic waves within the cylinder. Therefore, frequency-domain analysis provides a more physically meaningful approach to identify and characterize knock behavior. In this study, Fast Fourier Transform (FFT) is applied to high-resolution in-cylinder pressure signals to identify knock frequencies, quantify knock intensity, and improve knock detection reliability. Furthermore, a novel methodology based on FFT amplitude density comparison and dynamic windowing is proposed to enhance knock detection accuracy, particularly for hydrogen combustion, which exhibits high cycle-to-cycle variability.

5.1. FFT-Based Identification of Knock Frequency Using Gaussian Windowing

Fast Fourier Transform (FFT) is used to convert the in-cylinder pressure signal from the crank angle domain into the frequency domain, enabling identification of dominant frequency components associated with combustion chamber resonance and knock oscillations. Since knock is a localized high-frequency phenomenon occurring within a specific crank angle region, the pressure signal is first windowed before applying the FFT. A Gaussian window function is employed to isolate the knock-prone region while minimizing spectral leakage. The Gaussian window is defined as:

$$w(\theta) = \exp\left(-\frac{1}{2}\left(\frac{\theta - \theta_c}{\sigma}\right)^2\right) \quad (1)$$

where θ is the crank angle, θ_c is the window center location, and σ controls the window width (standard deviation). The windowed pressure signal is then calculated as:

$$P_w(\theta) = P(\theta) \cdot w(\theta) \quad (2)$$

where $P(\theta)$ represents the measured in-cylinder pressure signal and $P_w(\theta)$ is the Gaussian-windowed pressure signal. The discrete FFT of the windowed signal is computed as:

$$F(k) = \sum_{n=0}^{N-1} P_w(\theta_n) \cdot e^{-i2\pi kn/N} \quad (3)$$

where N is the total number of samples and k is the frequency index. The frequency axis is defined as:

$$f(k) = \frac{k}{N} f_s \tag{4}$$

where f_s is the sampling frequency. The sampling frequency used in the experiments is selected based on the engine speed (1100 rpm) and the requirements of crank-angle (0.1 crank angle) resolved data acquisition, ensuring sufficient temporal resolution for capturing high-frequency pressure oscillations associated with knock. Since the analysis is performed over multiple consecutive combustion cycles, the FFT magnitude is computed for each individual cycle and subsequently averaged to obtain a statistically representative frequency spectrum:

$$\overline{A}(k) = \frac{1}{N_c} \sum_{j=1}^{N_c} \left| F_j(k) \right| \tag{5}$$

where N_c is the number of analyzed cycles (1000 in this study) and $\overline{A}(k)$ represents the mean FFT amplitude at each frequency. Applying the FFT over the entire engine cycle may introduce frequency components unrelated to knock. Therefore, the selection of window parameters plays a critical role in accurate knock identification. The key parameters include window center location θ_c, window width σ, and the effective crank angle range covered by the Gaussian distribution. Proper selection ensures accurate identification of dominant knock frequencies and resonance amplitudes, whereas improper window placement can lead to attenuation of knock amplitude and incorrect frequency identification. During window selection, multiple window functions were evaluated, and the Gaussian window was selected based on its minimal spectral leakage characteristics and its ability to preserve the main signal energy while reducing distortion in the frequency domain.

Figure 5 illustrates the in-cylinder pressure signal, Gaussian window, and windowed pressure signal (left), along with the corresponding FFT modulus and frequency histogram (right). Figure 6 demonstrates the influence of window width and window center selection on the calculated FFT amplitude. As shown in Figure 6 (left), increasing the window width can introduce greater signal leakage in the FFT modulus calculation; however, the most stable and representative FFT amplitude was obtained at a window range of approximately 90°. Reducing the window width below 90° does not significantly affect the calculation, provided that the knock event remains fully captured within the selected window. The window should not be too narrow, as this may exclude part of the knock event, nor too wide, as excessive width can introduce non-knock-related components and increase spectral leakage. Similarly, the selection of window center location strongly influences the FFT amplitude in the knock frequency range (6–9 kHz). When the window center is positioned well before TDC, the FFT amplitude in the knock frequency band is relatively low. As the window center shifts toward TDC and slightly after TDC, a higher FFT amplitude is observed within the knock frequency range. This confirms the importance of selecting an appropriate window width and center location, as illustrated in Figure 6 (right).

5.2. Validation of Knock Frequency Using KP-PK Comparison

To validate the FFT-based knock frequency identification, the FFT amplitude spectrum is compared with the conventional online knock indicator (KP_PK). During knock events, the amplitude of specific frequency components increases significantly due to resonance amplification. It is observed that cycles with higher (KP_PK) values consistently show higher FFT amplitude at specific frequency bands. As shown in Figure 7, the FFT amplitudes have been classified according to the base KP_PK parameters; this confirms that knock is associated with excitation of natural acoustic frequencies of the combustion chamber.

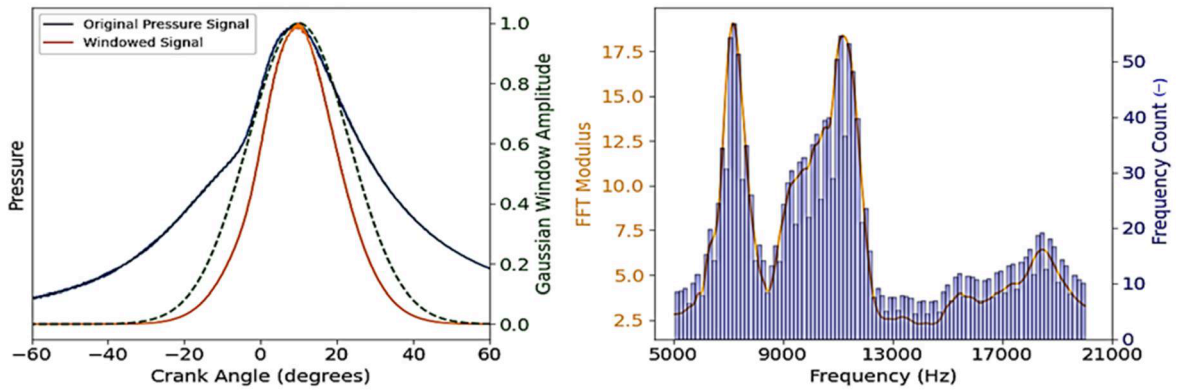

Figure 5. (**Left**)—In-cylinder pressure signal, Gaussian window, and windowed pressure signal; (**Right**)—FFT modulus (line plot) and frequency count (histogram).

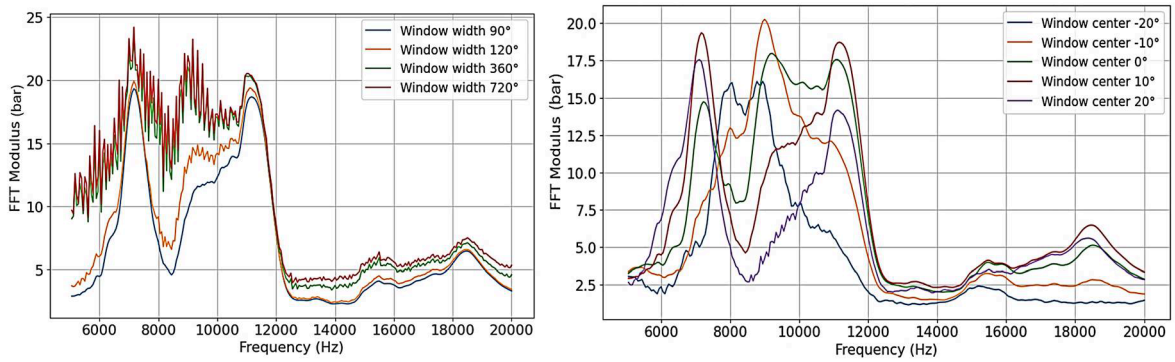

Figure 6. (**Left**)—effect of FFT window width selection; (**Right**)—effect of FFT window center location on amplitude variation.

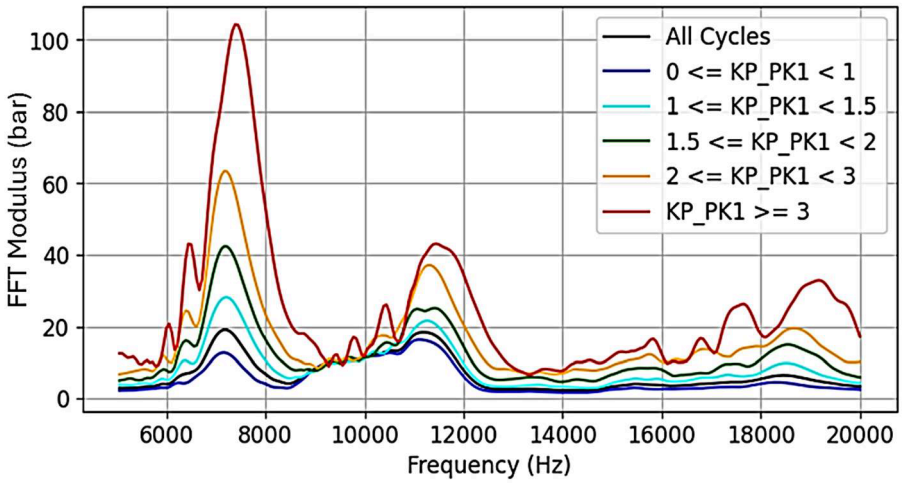

Figure 7. Variation of FFT amplitude with increasing knock intensity indicator (KP-PK).

This comparison provides independent confirmation of knock frequency and validates the use of FFT as a reliable knock detection tool.

5.3. Novel Knock Detection Using Stationary Window-Based FFT Density Method

The novelty of this study lies in evaluating knock intensity through comparison of resonance energy obtained from two fixed Gaussian window centers. Based on the FFT formulation described in Section 5.1, the windowed pressure signal is transformed into the frequency domain and the resonance amplitude within the knock-sensitive frequency

band is quantified. Instead of using only peak FFT amplitude, the resonance amplitude is calculated by integrating the FFT modulus over a predefined knock frequency range:

$$R(\theta_c) = \int_{f_{min}}^{f_{max}} |F_{\theta_c}(f)|\, df \tag{6}$$

where $R(\theta_c)$ = resonance amplitude at window center θ_c, f_{min} and f_{max} = knock-sensitive frequency range (4–20 kHz for stationary case), and $|F_{\theta_c}(f)|$ = FFT modulus of the windowed signal centered at θ_c. In the stationary method, two fixed window centers are selected as θ_c is 0° ATDCf and 10° ATDCf. The knock-sensitive frequency band is slightly refined to 4 kHz $\leq f \leq$ 20 kHz; this ensures better isolation of the structural resonance frequencies observed experimentally. For each cycle, resonance amplitudes are again computed using Equation (6), and the knock criterion remains $R10, j > R0, j$. This criterion is based on the physical understanding that knock-induced pressure oscillations are more intense shortly after TDC compared to the pre-TDC reference window. The calculated resonance amplitudes for all 1000 cycles are plotted together with the online knock indicator KP_PK. The cycles satisfying $R10 > R0$ are marked and compared against cycles where KP_PK > 2. The sensitivity of the proposed method is influenced by the selection of the window center. Because hydrogen combustion exhibits strong cycle-to-cycle variations in combustion phasing, a fixed (stationary) window center may not always coincide with the actual timing of resonance excitation. This misalignment can lead to overestimation or misclassification of knock cycles if the spectral window does not properly capture the dominant oscillatory event. To address this, two FFT-based spectral density values are calculated for each cycle: (i) a reference spectral density evaluated in a non-knock region (e.g., window center at TDC firing, denoted WC0), and (ii) a knock-region spectral density evaluated in a knock-prone region (e.g., window center at TDC firing + 10° CA, denoted WC10).

The integrated knock-band spectral amplitudes corresponding to these window centers are defined as $R10, j > R0, j$, respectively. The results of the FFT density analysis are presented in Figure 8. The top plot illustrates the cycle-resolved variation of resonance amplitudes, comparing $R0, j$ (WC0) and $R10, j$(WC10). The secondary y-axis shows the corresponding KP_PK values for comparison. This visualization highlights the relationship between the conventional peak-based knock indicator and the proposed spectral resonance-based criterion. The bottom plot is constructed after filtering all cycles using the proposed resonance-based condition $R10, j > R0, j$. Cycles that satisfy both the conventional condition (KP_PK > 2) and the resonance condition are marked in red, indicating confirmed resonance amplification in the knock-prone region. Cycles that satisfy only the resonance condition are shown in gray. Out of the total 1000 analyzed cycles, 120 cycles are identified as knock events based on the resonance-based condition. When this condition is satisfied, the corresponding cycle is classified as a knock cycle. However, the stationary window selection method still results in a higher number of detected knock cycles, leading to an overestimation of knock events. Therefore, this method can be further improved through a more appropriate window selection strategy.

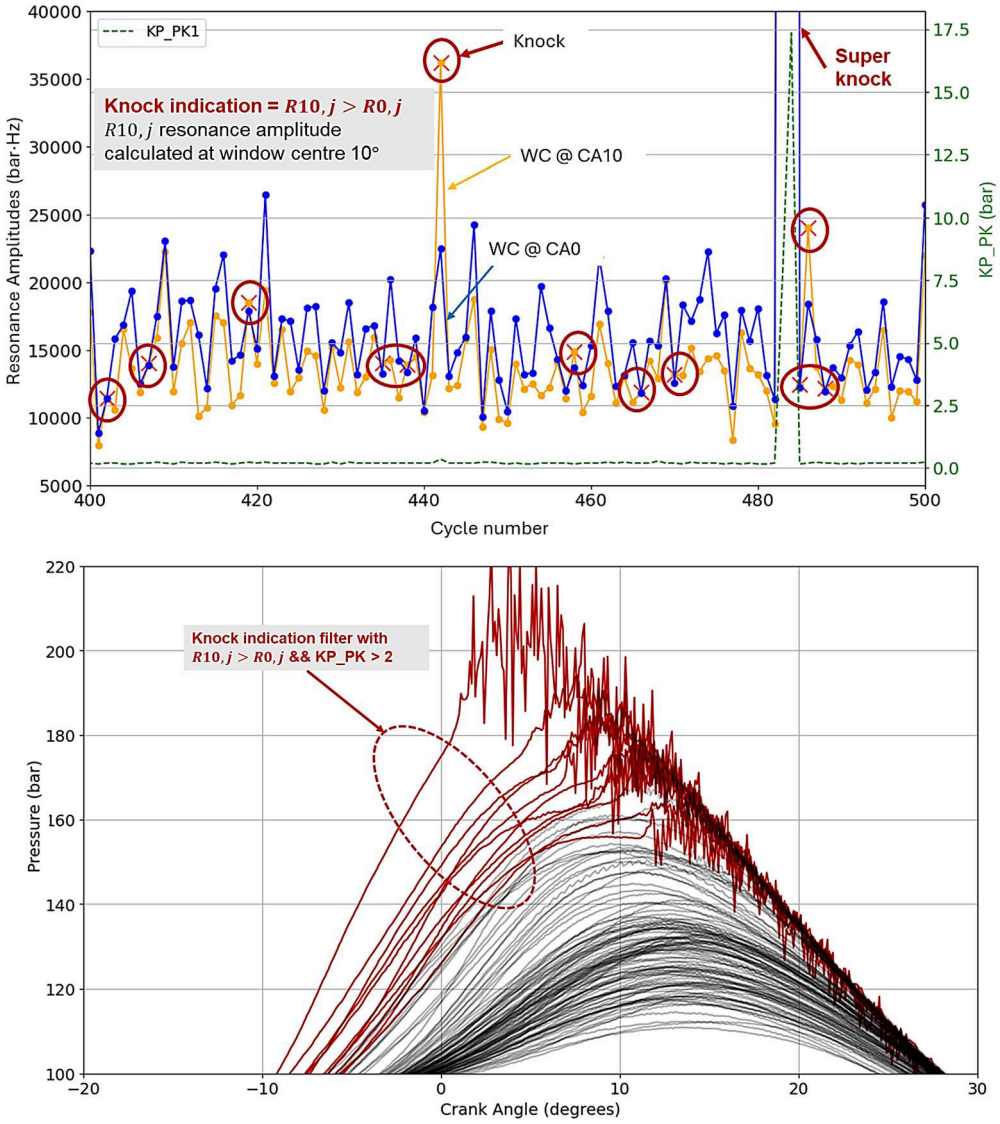

Figure 8. Resonance amplitude variation obtained from FFT-based spectral density analysis using fixed combustion-centered window positions at 0° and 10° ATDCF. The upper plot shows cycle-resolved resonance amplitude variation, while the secondary y-axis represents the online knock indicator KP_PK1. The lower plot highlights the identified knocking cycles based on resonance amplitude thresholding and corresponding in-cylinder pressure traces.

5.4. Dynamic FFT Window Method Based on Combustion Phasing (Novel Contribution)

To address the limitations of stationary window positioning, a dynamic FFT window selection method is proposed. Instead of fixing the window center at constant crank angles, the window center and width are defined using cycle-averaged combustion parameters: θ_{c1} = MFB10 (mass fraction burn at 10CA) and θ_{c2} = MFB50 (mass fraction burn at 50CA), and window width is combustion duration CA95. The knock-sensitive frequency band is slightly refined to 4 kHz $\leq f \leq$ 20 kHz to better isolate structural resonance frequencies observed experimentally. For each cycle, resonance amplitudes are again computed using the knock criterion $R\theta c2, j > R\theta c1, j$. Because the window location now follows combustion phasing, this method more accurately captures the true knock-prone region. When applied to 1000 measured cycles, the stationary method detected approximately 120 knock cycles and the dynamic window method reduced this number to approximately 30 cycles, as shown in Figure 9. This significant reduction demonstrates that many cycles previously classified as knock were artifacts of improper window alignment rather than true abnor-

mal combustion. Comparison of the identified cycles with pressure traces confirms that the dynamically selected window provides more realistic knock identification. Furthermore, correlation with the online KP_PK indicator improves when dynamic windowing is employed. The results confirm that incorporating combustion phasing (MFB: CA05, CA50, CA95) into FFT window positioning enhances physical consistency and reduces false-positive knock detection, particularly in hydrogen engines characterized by high combustion variability.

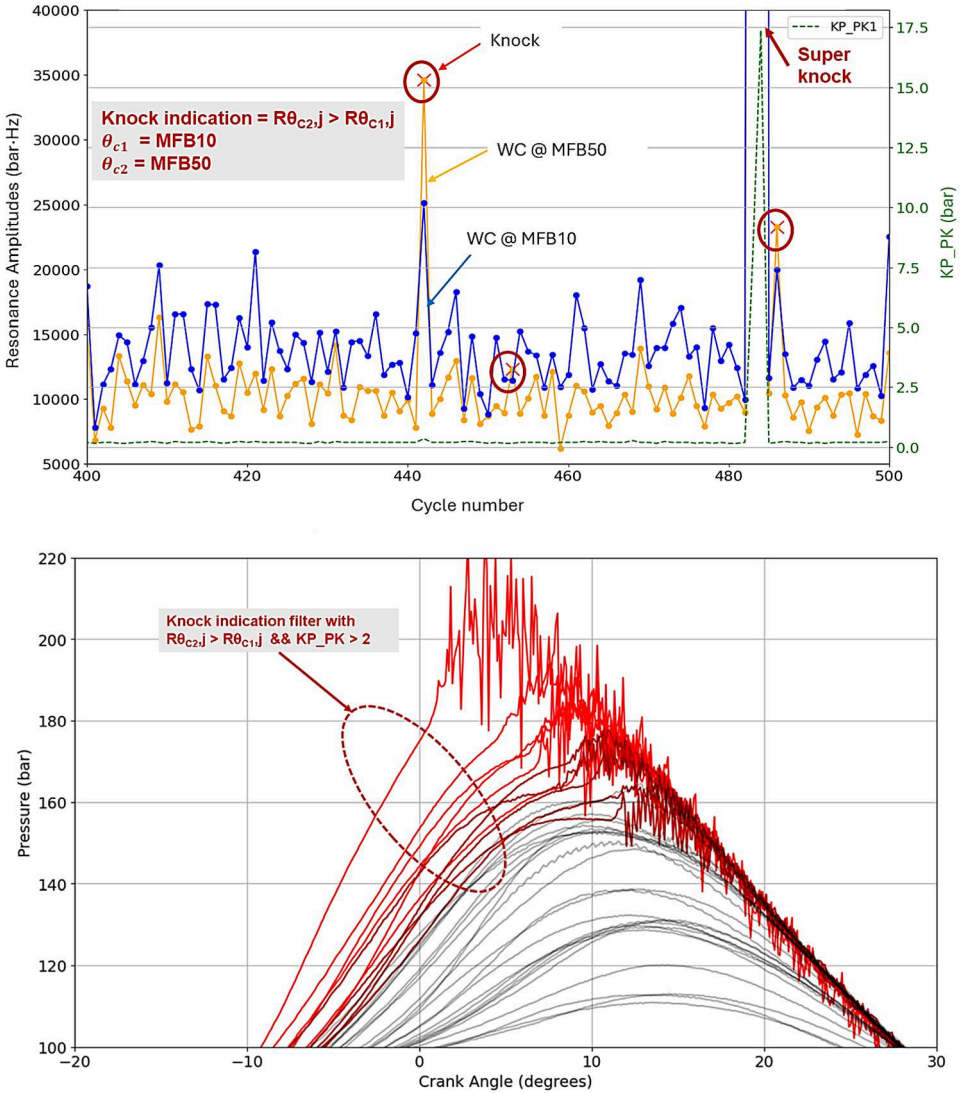

Figure 9. Resonance amplitude variation based on dynamically selected window centers determined from cycle-to-cycle variations of CA10 and CA50. The upper plot shows improved knock detection sensitivity compared to fixed-window analysis, while the lower plot presents the corresponding in-cylinder pressure traces for detected knock cycles. This adaptive windowing approach provides more realistic identification of transient knock events.

5.5. Advantages of the Proposed FFT-Based Knock Detection Method

The proposed FFT-based methodology offers significant improvements over conventional knock detection techniques. By analyzing the pressure signal in the frequency domain, the method allows for accurate identification of the dominant knock frequencies, which is critical for understanding the combustion behavior in hydrogen-fueled engines. In addition to accurate frequency identification, the method enhances knock detection sensitivity and reduces the likelihood of false knock detection caused by normal combus-

tion oscillations. This capability ensures that knock events are distinguished clearly from high-amplitude fluctuations that are part of regular combustion processes. Another key advantage is the improved reliability compared to conventional knock indicators such as maximum pressure rise, MAPO, or KP_PK, which can be inconsistent under varying operating conditions. The use of a dynamic FFT window further strengthens the method's performance, enabling it to adapt to the high cycle-to-cycle variability characteristic of hydrogen combustion. Overall, this frequency-domain approach forms a solid foundation for further knock characterization and enables advanced time–frequency analysis using Short-Time Fourier Transform (STFT), which is discussed in the following section.

6. Selective Sampling Filtration Method for Accurate Knock Amplitude Measurement

Accurately quantifying knock amplitude is critical for understanding the severity of abnormal combustion and its potential impact on engine components. While conventional time-domain knock indicators such as $\left(A_{\{osc\}}\right)$, IMPG, or KP-PK provide an estimate of knock intensity, they often overestimate or underestimate the true knock amplitude due to the contribution of other frequency components unrelated to knock. In hydrogen-fueled engines, where combustion exhibits high cycle-to-cycle variability and broad frequency content, this limitation becomes more pronounced. To address this issue, a Selective Sampling Filtration (SSF) method is proposed to measure knock amplitude more accurately based on frequency-domain analysis.

6.1. Concept of Selective Sampling Filtration

The SSF method is based on the principle that knock is associated with specific resonance frequencies determined by combustion chamber geometry and acoustic wave propagation. In the frequency spectrum obtained using Fast Fourier Transform (FFT), knock manifests as distinct peaks within defined frequency bands. Other frequency components correspond to non-knock phenomena such as normal combustion or background noise. The combined knock intensity would sometimes be much higher than the actual knock produced due to combustion anomalies. As shown in Figure 3 above, the maximum knock amplitude is almost 30 bars.

The SSF method isolates knock-related frequency components through the following procedure:

1. The in-cylinder pressure signal is first windowed using the dynamic FFT windowing method to isolate the knock-prone crank angle region.
2. The FFT amplitude spectrum is computed for the windowed signal.
3. Dominant knock frequencies are identified by detecting local maxima and their corresponding frequency boundaries.
4. Frequency components outside the identified knock bands are selectively removed.
5. The filtered signal is reconstructed using inverse FFT.
6. The knock amplitude is determined from the reconstructed pressure oscillations.

This selective filtration ensures that only knock-relevant frequency components contribute to the final amplitude measurement.

6.2. Mathematical Formulation

Let F(f) denote the FFT spectrum of the windowed pressure signal obtained from Section 5. The knock-sensitive frequency range is first restricted to 4000 Hz $\leq f \leq$ 20,000 Hz. Within this band, local maxima corresponding to resonance peaks are detected. For each dominant peak at frequency $fpeak$, the nearest surrounding local minima are identified: $fmin < fpeak < fmax$. These bounding minima define the natural bandwidth of the

corresponding acoustic resonance mode. Unlike fixed-band filtering, this approach adapts to cycle-to-cycle spectral variations and captures the true physical extent of each resonance peak.

In addition, the selection of the sampling frequency is guided by the theoretically possible resonance frequencies of the combustion chamber. According to Draper's equation, the fundamental acoustic resonance frequency of a cylindrical combustion chamber can be approximated as:

$$f_{n,m,p} = \frac{c}{2\pi}\sqrt{\left(\frac{\alpha_{n,m}}{R}\right)^2 + \left(\frac{p\pi}{L}\right)^2} \tag{7}$$

where c is the speed of sound in the cylinder gas, R is the cylinder radius, L is the cylinder length, $\alpha_{n,m}$ is the m-th root of the Bessel function of order n, and p is the longitudinal mode number along the cylinder axis. The experimentally selected sampling frequency ensures that all significant resonance modes predicted by Draper's equation are captured within the digitized signal, as shown in Figure 10, providing adequate resolution of the knock-sensitive spectral content. By combining FFT-based peak detection with theoretical mode estimation, this method robustly identifies the relevant acoustic resonances for knock analysis.

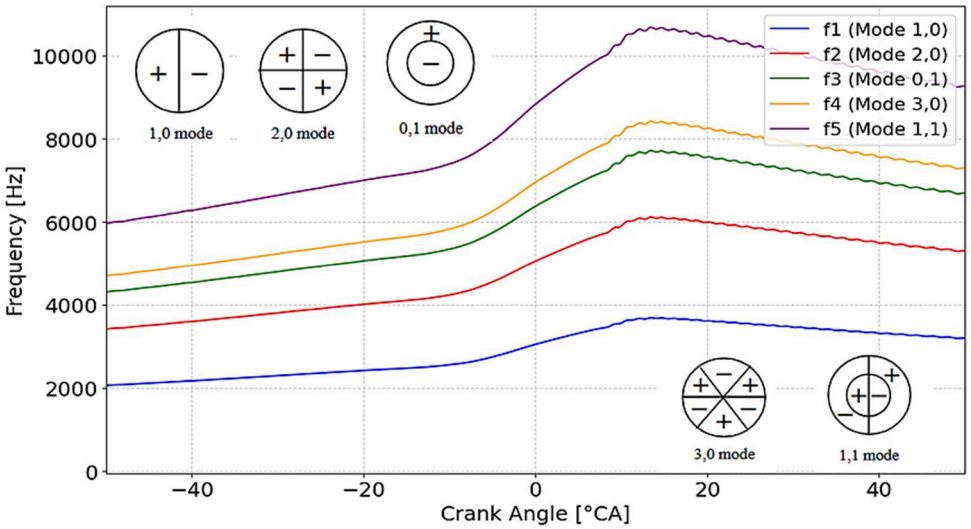

Figure 10. Resonance frequency modes predicted by Draper's equation.

Following the identification of dominant resonance peaks, a Selective Sampling Filtration (SSF) approach is applied to isolate the contribution of knock-related frequency bands. As shown in Figure 11 (Right), local maxima corresponding to resonance peaks are identified within the knock-sensitive frequency range, and the nearest surrounding minima define the natural bandwidth limits $fmin$ and $fmax$. These knock-prone frequency zones are indicated by dashed lines. The selective removal of a given resonance band is performed according to:

$$F_{\text{modified}}(f) = \begin{cases} 0, & \text{for } f_{min} \leq |f| \leq f_{max} \\ F(f), & \text{otherwise} \end{cases} \tag{8}$$

where the spectral components between $fmin$ and $fmax$ are set to zero, while all other frequency components remain unchanged. This ensures that only the targeted resonance

contribution is eliminated without affecting the remaining spectral content. The modified spectrum is then transformed back into the crank-angle domain using inverse FFT:

$$P_{\text{reconstructed}}(\theta) = \text{IFFT}\{F_{\text{modified}}(f)\} \tag{9}$$

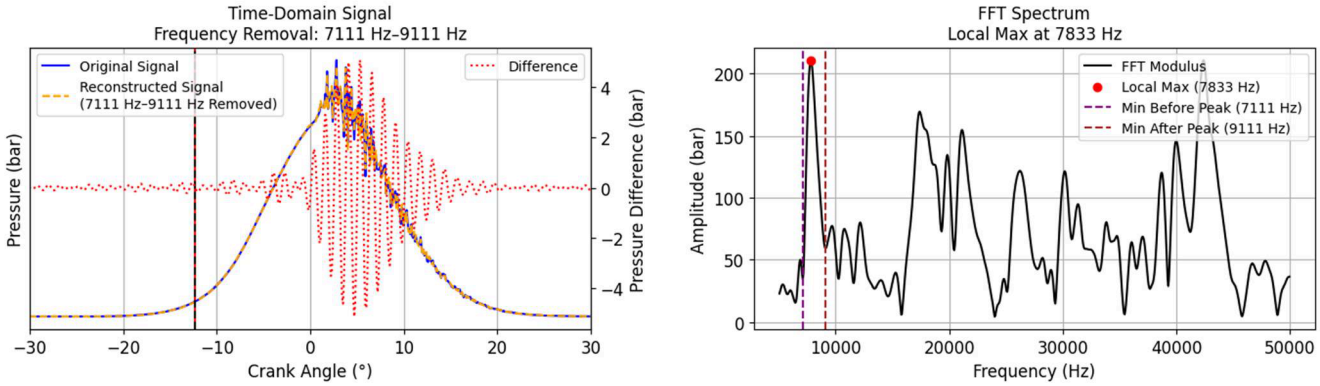

Figure 11. (**Right**)—FFT amplitude versus frequency with local maxima and minima indicated; knock-prone frequency zones marked with dashed lines. (**Left**)—reconstructed pressure signal obtained by removing knock frequencies, original pressure signal, and difference pressure on the secondary y-axis.

The resulting reconstructed signal represents the pressure trace with the selected knock frequency band removed. To quantify the oscillatory contribution of the removed resonance, the difference between the original windowed pressure signal $Pw(\theta)$ and the reconstructed signal is computed:

$$P_{\text{difference}}(\theta) = P_w(\theta) - P_{\text{reconstructed}}(\theta) \tag{10}$$

This difference signal isolates the pressure oscillations associated exclusively with the removed frequency band. The amplitude contribution of that specific resonance mode is determined using the peak-to-peak definition:

$$A_{\text{band}} = \max(P_{\text{difference}}(\theta)) - \min(P_{\text{difference}}(\theta)) \tag{11}$$

This process is repeated for all dominant resonance peaks identified in the spectrum. After isolating all knock-related frequency components, the final knock amplitude is determined from the reconstructed knock-only signal:

$$A_{\text{knock}} = \max(P_{\text{knock}}(\theta)) - \min(P_{\text{knock}}(\theta)) \tag{12}$$

Figure 11 (Left) illustrates the physical interpretation of this method. The original pressure signal, the reconstructed signal after knock frequency removal, and the difference pressure signal (shown on the secondary y-axis) are presented simultaneously. A noticeable reduction in high-frequency oscillations is observed after removing knock-prone frequency bands, confirming their direct contribution to pressure oscillation amplitude.

This selective filtration approach reduces overestimation of knock intensity by excluding non-knock frequencies, quantifies the contribution of individual resonance modes, and improves the accuracy of knock amplitude estimation under highly variable hydrogen combustion conditions. Application of the method over 1000 engine cycles demonstrated that conventional FFT or KP_PK approaches overestimated knock amplitude by 4–10 bar in several cycles, whereas the SSF method aligned closely with observed pressure oscillations.

Additionally, the analysis of each frequency band's contribution enables identification of specific resonance modes responsible for knock, providing insights for combustion optimization or hardware design. By combining selective filtration with dynamic FFT windowing, this method forms a robust framework for accurate, cycle-resolved knock amplitude estimation and serves as a foundation for subsequent time–frequency analysis and precise determination of knock timing and duration.

7. Time–Frequency Analysis Using Short-Time Fourier Transform (STFT)

While frequency-domain analysis using FFT identifies knock frequencies and amplitudes, it does not provide information on when knock events occur during the engine cycle. In hydrogen-fueled engines, knock is highly transient and occurs within a narrow crank angle window. To capture both the temporal and spectral characteristics of knock, Short-Time Fourier Transform (STFT) is applied to the Gaussian-windowed in-cylinder pressure signal. STFT is implemented using the Python "scipy.signal.stft" function. Mathematically, the discrete STFT of the windowed signal $Pw[n]$ can be expressed as:

$$STFT[m,k] = \sum_{n=0}^{N-1} P_w[n] \cdot w[n - mR] \cdot e^{-i2\pi kn/N} \tag{13}$$

where $P_w[n]$ is the Gaussian-windowed pressure signal, w[n] is the Hann window applied during STFT segmentation, N is the segment length (nperseg in code), R = N−noverlap is the hop size, k is the frequency bin index, and m is the segment index corresponding to each time (crank angle) window. The selected window parameters were determined based on minimum spectral leakage, reduced signal loss, and the best agreement between the STFT and FFT spectral responses. The STFT produces a complex-valued spectrogram $Z[m,k]$, representing the amplitude and phase of each frequency component as it evolves along the crank angle axis. The amplitude of each frequency bin is obtained as:

$$|STFT[m,k]| = \sqrt{Re\{STFT[m,k]\}^2 + Im\{STFT[m,k]\}^2} \tag{14}$$

In this study, the mean amplitude over all time segments is calculated to quantify the average spectral content for each cycle:

$$\overline{A}(k) = \frac{1}{M} \sum_{m=0}^{M-1} |STFT[m,k]| \tag{15}$$

where M is the number of overlapping time windows.

Identification of Knock Timing and Duration

The STFT spectrogram allows the identification of crank angle ranges where knock occurs. Knock onset is defined as the first crank angle θ where the STFT amplitude exceeds a threshold, and knock duration is the span over which the amplitude remains above that threshold: $KnockOnset = \min\{\theta \mid |STFT(\theta, f)| > Threshold\}$ and $KnockDuration = \theta_{end} - \theta_{start}$. The resonance amplitude within the knock-sensitive frequency band (4–20 kHz) is also evaluated by integrating the STFT amplitude over the selected frequency range at each crank angle:

$$R(\theta) = \int_{f_{min}}^{f_{max}} |STFT(\theta, f)|\, df \tag{16}$$

This provides a time-resolved measure of the strength of knock-related oscillations along the crank angle axis. Figure 12 presents the results of the Short-Time Fourier Trans-

form (STFT) analysis applied to the windowed in-cylinder pressure signal. In the top panel, the mean FFT amplitude is compared with the mean STFT amplitude within the knock-sensitive frequency range of 4–20 kHz. While FFT provides the overall spectral content, STFT captures temporal variations of the spectral components, revealing how the amplitude of specific frequencies evolves along the crank angle. The bottom panel shows the evolution of the maximum resonance amplitude in the crank-angle domain along with the theoretical resonance frequency modes. The color plot of STFT amplitude indicates that knock events are most pronounced around CA10, and the dominant modes corresponding to f3(0,1) and f4(3,0) are primarily responsible for the resonance at approximately 7800 Hz. Similar analyses can be performed for other combustion cycles to evaluate cycle-to-cycle knock behavior. This representation clearly identifies the precise crank angle locations of knock events, providing temporal localization that cannot be obtained from stationary FFT analysis alone. By combining frequency and time information, the STFT-based approach allows simultaneous determination of knock frequency, amplitude, timing, and duration. Such a time–frequency representation is particularly valuable for hydrogen-fueled engines, where combustion is highly transient and knock events vary significantly between cycles. Overall, this approach enables detailed characterization of knock onset and duration, providing a robust framework for assessing the transient nature of knock in each engine cycle.

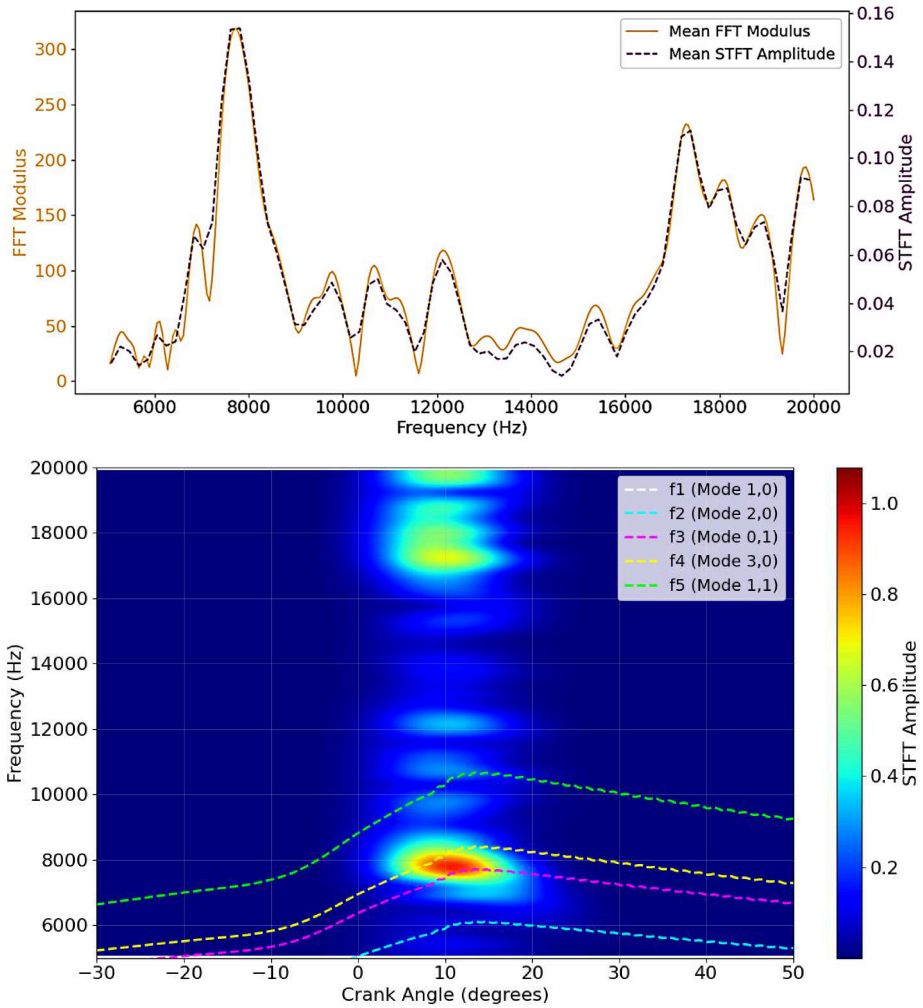

Figure 12. (**Top**)—comparison of FFT and STFT amplitudes; (**Bottom**)—location of maximum resonance amplitude (normalized) in time and frequency domains shown with theoretical resonance frequencies.

8. Conclusions

This research explored the knock phenomenon in hydrogen-fueled spark-ignition engines by integrating advanced signal processing, spectral analysis, and theoretical modeling. The study highlights the challenges and opportunities in accurately detecting and quantifying knock, especially under the fast flame speed and detonation-prone characteristics of hydrogen.

Key findings:

- Conventional knock detection methods, such as MAPO and simple FFT-based approaches, are limited and do not fully capture cycle-to-cycle variations or the complexities of resonance.
- Online knock detection provides real-time monitoring but can be affected by noise and engine transients, whereas offline methods allow detailed spectral analysis and post-processing refinement.
- When properly applied, FFT-based analysis matches conventional knock indicators, provided that window width and center are carefully selected to resolve knock-sensitive frequencies without spectral leakage, especially in high-speed hydrogen-fueled engines.
- A novel knock detection method using discrete FFT (DFFT) applied at carefully selected stationary Gaussian window points improves the sensitivity and accuracy of knock identification by targeting the pressure signal at the expected combustion location.
- The approach is further enhanced by dynamic Gaussian windowing based on mass fraction burned and combustion duration, which captures cycle-to-cycle variations more effectively, leading to more accurate knock counts and providing a reliable parameter for engine development and control strategy optimization.
- Selective sampling and filtering techniques further enable detailed analysis of the absolute knock oscillation amplitude caused by combustion events, while minimizing interference from other natural frequencies of the engine, sensors, or actuators.
- Short-Time Fourier Transform (STFT) helps to understand knock events in both time and frequency domains, and combined with Draper's equation, it allows identification of the dominant resonance modes during specific combustion events.

In conclusion, the proposed approach combining adaptive spectral analysis, dynamic windowing, and theoretical modeling offers a robust framework for detecting and characterizing knock in hydrogen engines. This methodology not only overcomes limitations of conventional techniques but also enables accurate, cycle-resolved monitoring, providing a foundation for improved engine calibration and advanced knock control strategies.

Author Contributions: B.K.: Writing—original draft, Software, Visualization, Investigation, Formal analysis, Conceptualization. U.W.: Writing—review and editing, Supervision. T.K.: Writing—review and editing, Supervision. All authors have read and agreed to the published version of the manuscript.

Funding: This research was funded by the Federal Ministry for Economic Affairs and Energy, grant number 19I24003F. Open access funding was provided by the Karlsruhe Institute of Technology (KIT) through the Institutional Open Access Program (IOAP) of the Helmholtz Association.

Data Availability Statement: No new data were created or analyzed in this study. Data sharing is not applicable to this article.

Acknowledgments: The authors express their gratitude to the Federal Ministry for Economic Affairs and Energy for funding this work within the project PoWer following a decision of the German Bundestag.

Conflicts of Interest: The authors declare that they have no known competing financial interests or personal relationships that have influenced the work reported in this paper.

Abbreviations

The following abbreviations are used in this manuscript:

Abbreviation	Full Form
CA	Crank Angle
DKI	Derivative Knock Index
FFT	Fast Fourier Transform
DFFT	Discrete Fast Fourier Transform
STFT	Short-Time Fourier Transform
SSF	Stationary Selection Filter
KP_PK	Knock Peak-to-Peak
MAPO	Maximum Amplitude of Pressure Oscillation
IMPG	Integrated Magnitude of Pressure Gradient
IMPO	Integrated Magnitude of Pressure Oscillation
WC0	Window Center 0°
WC10	Window Center 10°
TDC	Top Dead Center
PSD	Power Spectral Density
R0	Resonance amplitude at WC0
R10	Resonance amplitude at WC10
f_{peak}	Peak frequency
fmin/fmax	Bounding minima
CA10	Crank Angle 10°
zeta (ζ)	Normalization factor
PW	Pressure Window
$\Delta\theta/d\theta$	Crank Angle Increment

References

1. Jayaprabakar, J.; Arunkumar, T.; Rangasamy, G.; Parthipan, J.; Anish, M.; Varshini, G.; Kumar, B.K. Prospectus of hydrogen enrichment in internal combustion engines: Methodological insights on its production, injection, properties, performance and emissions. *Fuel* **2024**, *363*, 131034. [CrossRef]
2. Liang, B.; Cheng, L.; Zhang, M.; Huang, Y.; Wang, J.; Liu, Y.; Ma, F.; Huang, Z. Effects of chamber geometry, hydrogen ratio and EGR ratio on the combustion process and knocking characters of a HCNG engine at the stoichiometric condition. *Appl. Energy Combust. Sci.* **2023**, *15*, 100189. [CrossRef]
3. Kurtz, J.; Sprik, S.; Bradley, T.H. *Review of Transportation Hydrogen Infrastructure Performance and Reliability*; Elsevier Ltd.: Amsterdam, The Netherlands, 2019. [CrossRef]
4. Kim, J.; Chun, K.M.; Song, S.; Baek, H.K.; Lee, S.W. Hydrogen effects on the combustion stability, performance and emissions of a turbo gasoline direct injection engine in various air/fuel ratios. *Appl. Energy* **2018**, *228*, 1353–1361. [CrossRef]
5. Wang, H.; Ji, C.; Shi, C.; Wang, S.; Yang, J.; Ge, Y. Investigation of the gas injection rate shape on combustion, knock and emissions behavior of a rotary engine with hydrogen direct-injection enrichment. *Int. J. Hydrogen Energy* **2021**, *46*, 14790–14804. [CrossRef]
6. Shao, J.; Rutland, C.J. Modeling Investigation of Different Methods to Suppress Engine Knock on a Small Spark Ignition Engine. *J. Eng. Gas Turbines Power* **2015**, *137*, 061506. [CrossRef]
7. Zhen, X.; Wang, Y.; Xu, S.; Zhu, Y.; Tao, C.; Xu, T.; Song, M. *The Engine Knock Analysis—An Overview*; Elsevier Ltd.: Amsterdam, The Netherlands, 2012. [CrossRef]
8. Szwaja, S.; Naber, J.D. Dual nature of hydrogen combustion knock. *Int. J. Hydrogen Energy* **2013**, *38*, 12489–12496. [CrossRef]
9. Li, Y.; Gao, W.; Li, Y.; Fu, Z.; Zou, J. Numerical investigation on combustion and knock formation mechanism of hydrogen direct injection engine. *Fuel* **2022**, *316*, 123302. [CrossRef]
10. Brecq, G.; Bellettre, J.; Tazerout, M. A new indicator for knock detection in gas SI engines. *Int. J. Therm. Sci.* **2003**, *42*, 523–532. [CrossRef]
11. Bares, P.; Selmanaj, D.; Guardiola, C.; Onder, C. A new knock event definition for knock detection and control optimization. *Appl. Therm. Eng.* **2018**, *131*, 80–88. [CrossRef]

12. Luo, Q.H.; Sun, B.G. Inducing factors and frequency of combustion knock in hydrogen internal combustion engines. *Int. J. Hydrogen Energy* **2016**, *41*, 16296–16305. [CrossRef]
13. Lee, J.-H.; Hwang, S.-H.; Lim, J.-S.; Jeon, D.-C.; Cho, Y.-S. A New Knock-Detection Method Using Cylinder Pressure, Block Vibration and Sound Pressure Signals from a SI Engine. 1998. Available online: https://about.jstor.org/terms (accessed on 1 June 2025).
14. Akimoto, K.; Komatsu, H.; Kurauchi, A. Development of pattern recognition knock detection system using short-time fourier transform. *IFAC Proc. Vol.* **2013**, *46*, 366–371. [CrossRef]
15. Vulli, S.; Dunne, J.F.; Potenza, R.; Richardson, D.; King, P. Time-frequency analysis of single-point engine-block vibration measurements for multiple excitation-event identification. *J. Sound Vib.* **2009**, *321*, 1129–1143. [CrossRef]
16. Bares, P.; Selmanaj, D.; Guardiola, C.; Onder, C. Knock probability estimation through an in-cylinder temperature model with exogenous noise. *Mech. Syst. Signal Process.* **2018**, *98*, 756–769. [CrossRef]
17. Chen, A.; Dai, X. Internal combustion engine vibration analysis with short-term Fourier-transform. In *2010 3rd International Congress on Image and Signal Processing*; IEEE: New York, NY, USA, 2010; pp. 4088–4091. [CrossRef]
18. Kozlov, A.; Terenchenko, A.; Zuev, N.; Zelentsov, A. CFD Simulation of Knock Onset in a Heavy-Duty Spark Ignition Gas Engine. *Int. J. Recent Technol. Eng. IJRTE* **2019**, *8*, 9587–9593. [CrossRef]